

Thermal Transition Properties of Spaghetti Measured by Differential Scanning Calorimetry (DSC) and Thermal Mechanical Compression Test (TMCT)

Mohammad Shafiur Rahman · Wijitha Senadeera ·
Ahmed Al-Alawi · Tuyen Truong · Bhesh Bhandari ·
Ghalib Al-Saidi

Received: 31 March 2009 / Accepted: 28 August 2009 / Published online: 16 September 2009
© Springer Science + Business Media, LLC 2009

Abstract Glass transition temperature (T_g) of spaghetti sample was measured by thermal and rheological methods as a function of water content from 0 to 70 kg/100 kg spaghetti. In the cases of sample containing un-freezable water (i.e., amount of water which did not form ice even at very low temperature), calorimetric measurements performed by differential scanning calorimetry showed that the T_g values decreased from 142.8 to 42.7°C when water content increased from 0 to 13.95 kg/100 kg spaghetti, respectively. Glass transition temperature increased with the increase of heating rate (2–50°C/min) and reached to a nearly constant value above 30°C/min. Thermal mechanical compression test showed relatively lower T_g values compared to the DSC values at low moisture contents, whereas at high moisture content T_g showed higher values. In the cases of samples containing freezable water (27–70 kg/100 kg spaghetti), glass transition shifts were merged with the ice melting endotherm. The freezing point, measured from the endothermic peak, decreased with the decrease of water content. In the state diagram, maximal freeze-concentration condition was determined as $X'_s=0.81$ kg/kg

spaghetti from the intersection of the extended freezing curve and a horizontal line passing thru $T'_m=-10.3$ °C.

Keywords Pasta · Starch · Glass transition temperature · Food thermal analysis · Fourier transform infrared (FTIR)

Introduction

Quality loss of foods is influenced by its storage and distribution conditions. These quality losses are categorized into: (1) microbiological growth, recovery, and death; (2) physical changes (i.e., texture, color); and (3) chemical/biological changes (i.e., nutritional composition) (Martins et al. 2008). Glass transition in foods could be used to determine its stability during storage. Glass transition concept emerged in food processing in the 1980s, when Levine and Slade (1986) and Slade and Levine (1988) identified its merits in food processing and stability during storage (Rahman 2006). Foods can be considered very stable at the glassy state, since below glass transition temperature compounds involved in the deterioration reactions take many months or even years to diffuse over molecular distances and approach each other to react (Slade and Levine 1991; Rahman 2009). Similarly, structural, mechanical, and transport properties could also be related with glass transition (Jaya and Das 2009). Glass transition is a nature of second-order time–temperature-dependent transition, which is characterized by a discontinuity or change in the slope of physical, mechanical, electrical, thermal, and other properties of a material when plotted as a function of temperature (Rahman 1995). A low glass transition means that, at room or mouth temperature, the food is soft and relatively plastic, and at higher temperatures it may even

M. S. Rahman (✉) · A. Al-Alawi · G. Al-Saidi
Department of Food Science and Nutrition, College of
Agricultural and Marine Sciences, Sultan Qaboos University,
P.O. Box 34, Al-Khod-123 Muscat, Oman
e-mail: shafiur@squ.edu.om

W. Senadeera
School of Engineering Systems,
Queensland University of Technology,
Brisbane QLD 4001, Australia

T. Truong · B. Bhandari
The University of Queensland, School of Land,
Crop and Food Sciences,
Brisbane QLD 4072, Australia

flow. In contrast, a food with a high glass transition temperature is hard and brittle at ambient temperature. Early attempts to describe glassy phenomena concluded that glass is a liquid that has lost its ability to flow in a short time frame, thus instead of taking the shape of its container, glass itself can serve as the container for liquids. Molecular mobility increases 100-fold above glass transition, thus foods are the most stable below its glassy state (Rahman 2010).

The most common method used to determine glass transition is the differential scanning calorimetry (DSC) which detects the change in heat capacity (i.e., a shift in the thermogram line) occurring over the two states (i.e., glassy and rubbery). Recently, modulated DSC is being used to increase the sensitivity and resolution of complex thermal events. The thermo-mechanical analysis (TMA, DMA, and DMTA) and oscillation methods are less commonly used; however, these methods are more sensitive (Bell and Touma 1996). The main reasons of the lower use of the thermo-mechanical methods are due to the complexity of these methods, difficulties in sample preparation, and the possibility of moisture loss during its measurement at high temperatures. In addition, the thermo-mechanical analysis is widely used to determine the structural and functionality of food products, for example Alvarez et al. (2009) measured the mechanical characteristics of fresh and frozen-thawed mashed potato by oscillatory rheometer. TMA measures the change of slope when geometric dimension is plotted against temperature, whereas DMTA and oscillation methods measure the storage and loss modulus as a function of temperature (Rahman et al. 2007).

The recent thermal mechanical compression test (TMCT) device, which was developed by Bhandari and co-workers at The University of Queensland (Australia), has the potential capability to measure the phase transition temperature of solid materials (Bhandari 2007). In this method, the sample is heated under compression using a probe attached to a texture analyzer. The mechanical softening of the sample at the interface of heating surface caused significant displacement at a specific temperature, and this transition is considered as the glass–rubber transition temperature. TMCT method has been proved to be simple, reproducible, and economical, and it was used to measure glass transition of numbers of high and low molecular weight dry food and non-food materials (Sablani et al. 2008; Boonyai et al. 2007).

Cremer and Kaletunc (2003) registered the FTIR spectra of corn- and oat-based extruded products. All spectra for corn- and oat-based products showed a broad peak in the region $3,600\text{--}3,000\text{ cm}^{-1}$, which is due to the —OH group stretching vibration in starch molecule. Protein in the starch-based products showed amide I and amide II bands which appear typically in the region $1,600\text{--}1,700\text{ cm}^{-1}$. The

location, shape, and intensity of these peaks indicated the structural changes in protein during processing (Wetzel 1993; Chittur 1998; Fabian and Schultz 2000; Kazemzadeh et al. 1982; van Dijk et al. 1997). The absorbance ratio of amide I and amide II also varied with the corn- and oat-based extruded products (Cremer and Kaletunc 2003).

The phase transition properties of a number of food materials have been reported in various research papers, while the glass transition properties of wheat-based products such as pasta and spaghetti have been reported rarely. Recently, Rahman et al. (2007) reported the glass transition of spaghetti at moisture content 9.77 kg/100 kg spaghetti. This was measured by mechanical, thermal, water diffusion, and density methods (Rahman et al. 2007). Based on the authors' knowledge, there is negligible information available for the glass transition of spaghetti at different moisture contents (Takhar et al. 2006; Cuq et al. 2003). Freezing point and maximal freeze-concentration condition are needed to develop the state diagram. The earlier stability map was developed based on the water activity concept (Rahman 2009). State diagram is another stability map indicating different states and phases of a food as a function of water or solids content and temperature (Roos 1995; Rahman 2004, 2006). Negligible work has been reported in the literature for thermal characteristics of spaghetti, which could be used to develop a state diagram for spaghetti. The objectives of this work were to measure the glass transition and freezing point of spaghetti as a function of different water content and to determine the maximal freeze-concentration condition. These characteristics of the spaghetti could be used to develop the state diagram, which can be used to determine the storage stability of spaghetti as a function of temperature and water content. In addition, optimum processing conditions for spaghetti manufacturing could be identified from the state diagram. The nature of bound water in the spaghetti matrix, which influences phase transition properties of spaghetti, were measured by Fourier transform infrared (FTIR) absorption as a function of moisture content at 20°C . The maximum stability of spaghetti during storage could be observed at the moisture content at or below the level of strongly bound water.

Materials and Methods

Material

Commercial spaghetti produced in Australia was purchased from a supermarket in Sydney. The ribbon-shaped spaghetti (suitable for mechanical analysis) was taken out from the pack and stored in an airtight glass bottle at experimental temperature (20 or 25°C) until used for the experiments. Moisture content (kg/100 kg spaghetti) of

the sample was determined from the solids content by drying spaghetti sample in an oven at 105°C for at least 18 h.

Sample Preparation with Different Water Content

The water sorption isotherm was determined at experimental temperature (i.e., 20°C) using an isopiestic method (Rahman and Sablani 2009). In this method, a weighted sample of known mass is stored in an enclosure and allowed to reach equilibrium with an atmosphere of known equilibrium relative humidity, for example, by a saturated salt solution, and reweighed at regular intervals until constant weight is established (Rahman and Sablani 2009). For this purpose, spaghetti samples were placed in open weighing bottles and stored in airtight glass jars while maintaining relative humidity equilibrium with saturated salt solutions (with a crystal layer visible at the bottom of jars). The salts used in the experiments were: LiCl, CH₃COOK, MgCl₂, K₂CO₃, NaBr, SrCl₂, and KCl (BDH, Laboratory Supplies, Poole, UK). Relative humidity values for these solutions were obtained from the review of Rahman and Sablani (2009). The jars were placed at room temperature. Thymol in a beaker was used in high water activity airtight jars to avoid microbial growth in the sample during equilibration period. After at least 3 weeks, the samples were taken out and stored at 5°C in airtight glass bottles. Samples containing water less than 4.88 kg/100 kg spaghetti were prepared by drying in an oven at 105°C for a predetermined time. Samples containing water at and above 27 kg/100 kg were prepared by adding a predetermined amount of water in the spaghetti and equilibrating the sample at a storage temperature of 5°C after placing them in an airtight glass bottle. For TMCT method, the spaghetti samples (cut in length of 6 cm) were equilibrated for at least 2 weeks in vacuum-sealed desiccators, maintained at different relative humidity with saturated salt solutions, at 25°C. The water content was determined by drying spaghetti in an oven at 105°C for 16 h. The range of moisture content used in this study varied from 0.0 to 70.0 kg/100 kg spaghetti. The equilibration temperatures were at 20°C for DSC method and 25°C for TMCT methods. This was due to the difference in room temperatures in Oman (for DSC) and Australia (for TMCT). However, this variation was clearly identified and moisture contents were presented with the measured glass transition temperatures by DSC and TMCT methods.

Thermal Transitions by DSC

A differential scanning calorimeter (Q10, TA Instruments, New Castle, DE, USA) was used to perform thermal experiments. Mechanical refrigerated cooling system was used to cool the sample until -90°C. The calorimeter was

calibrated by checking temperature and enthalpy of fusion of indium and water as high purity standards.

Sample Containing Un-freezable Water (i.e., Water Present in Spaghetti did not Form Ice Even at Low Temperature)

Equilibrated spaghetti samples (5–10 mg) prepared by isopiestic method at different water activities were placed in aluminum pans (capacity 30 μL) and were cooled to -90°C at the rate of 5°C/min, and kept for 10 min. In order to study the effect of heating rate, sample containing moisture of 10.2 kg/100 kg spaghetti were heated from -90 to 130°C at different rates in the range of 2–50°C/min, while samples with different moisture content were heated from -90 to 180°C at a heating rate of 20°C/min. Each thermogram was analyzed and onset (T_{gi}), middle (T_{gp}), and end (T_{ge}) of glass transition temperatures from a shift observed in the thermogram line. Three replicates were used for selected samples.

Sample Containing Freezable Water (i.e., Portion of Water in Spaghetti was Transformed into Ice at Low Temperature)

A different procedure was used for spaghetti (high water) containing freezable water. Samples of 10–20 mg (with high water contents from 27 to 70 kg/100 kg spaghetti) of spaghetti in a sealed aluminum pan were cooled to -90°C at 5°C/min, and remained for 10 min. They were then heated initially from -90 to 100°C at 10°C/min in order to determine apparent (T'_m)_a and (T''_g)_a, freezing point, and enthalpy of ice melting. Optimum annealing condition at [$(T'_m)_a - 1$] should be used in order to determine annealed T'_m and T''_g (Bai et al. 2001). Annealing time at [$(T'_m)_a - 1$] was varied from 0 to 4 h in order to find its effects on the annealed T'_m and T''_g . The ultimate maximal freeze-concentration condition was determined as T'_m and T''_g from the lowest moisture content spaghetti (27.0 kg/100 kg spaghetti) containing freezable water. The value of X'_s was determined in the state diagram (plot of temperature versus solids content) from the intersection of the extended freezing curve and a horizontal line passing thru ultimate T'_m and finally the value of X'_s was read on the x -axis.

Three transitions (peak, maximum slope, and start of melting) were determined from the ice melting endotherm. The initial or equilibrium freezing point was considered as the point of maximum slope of the endothermic peak as recommended by Rahman (2004). For the materials showing wide peak of ice melting on the DSC thermogram, the point of maximum slope corresponds well with the initial freezing point estimated from a widely accepted cooling curve method (Rahman 2004). The latent heat of ice melting or freezing was estimated from the area of the melting endotherm. The heating rate used for the spaghetti

samples with un-freezable water was at 20°C/min, close to the critical heating rate when glass transition reached to a constant value, whereas in the case of samples with freezable water it was used at 10°C/min in order to maximize the melting of ice formed during freezing process.

TMCT Method

The TMCT device is made up of an aluminum sample block (50×50×25 cm), which was thermally controlled by heater controller (BCT9300, Brainchild Electronic Co., Taipei, Taiwan) at a thermal scanning rate of 30°C/min. The data set of probe position, compression force at specific time, and temperature of sample cell were recorded by a 2-mm cylindrical probe and temperature probe attached to the texture analyzer TA.XTplus (Stable Microsystems, UK), respectively.

Preliminary work showed that more displacement was obtained if spaghetti is placed over the sample cell rather than inside the sample cell (which was a common practice with other samples such as rice grain or powder). The change of temperature in the sample surface in contact with heating surface caused mechanical softening and displacement at the middle of the spaghetti when force was applied. The temperature when a significant displacement occurred was considered as the glass transition temperature by TMCT and compared with the onset of DSC T_g values. Furthermore, the moisture loss can be minimized since the testing time was very short due to fast heating rate (30°C/min).

All tests were carried out under relaxation mode of texture analyzer. The data acquisition rate was 5 pps (points per second). The spaghetti was taken out from the desiccator and measured immediately to prevent any moisture loss or gain. The spaghetti was placed over the sample cell and allowed to hold under the 2-mm probe at the force of 0.49 N for 30 s before the thermal scanning. The sample was then scanned from room temperature to 140°C. During this thermal scanning, the displacement distances of the probe were recorded. All measurements were done in triplicate. The temperature vs. probe displacement was plotted to estimate the T_{g-r} (glass–rubber transition temperature) by performing linear regression as shown in Fig. 1. The T_{g-r} measured by TMCT corresponded to the T_{gi} of DSC method when the sample started to change from glassy state (i.e., end of glassy state) to rubbery state (i.e., start of rubbery state). However, TMCT method could not be used to measure T_{gp} and T_{ge} as determined by DSC method. In addition, DSC method could handle any form of sample such as powder and small piece, whereas only a specific geometric shape with a required dimension such as ribbon and bar could be used for TMCT method.

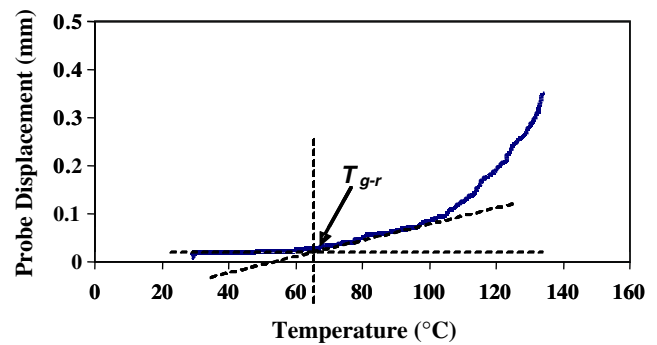


Fig. 1 Probe displacement versus temperature scan rate of 30°C/min showing a glass–rubber transition temperature (T_{g-r})

FTIR Analysis

The instrument used for this study was a Magan 560 FTIR spectrometer (Thermo Nicolet, USA) equipped with a deuterated triglycine sulfate detector and purged with dry air from a Balston dryer (Balston, Lexington, MA, USA). Before analysis, the spaghetti powder samples were sieved through a 250- μ m mesh. The fine particles were collected and immediately placed in a separate container. The collected powders were analyzed by placing them at the surface of a single-bounce ZeSe ATR crystal mounted on the sample compartment. The path length was controlled by applying constant pressure on the sample during scanning. All spectra were collected by co-adding 128 scans at a resolution of 4 cm^{-1} and a gain of 1.0. For quantification of moisture content, the peak height of the water $\nu(\text{HOH})$ bend band at 1,641 cm^{-1} was measured relative to a baseline point at 1,786 cm^{-1} .

Statistical Analysis

Selected points were replicated three times and their average values with its standard deviation were reported using Microsoft Excel. The modified Gordon–Taylor model parameters were estimated using SAS (2001) non-linear regression procedure.

Results and Discussion

The moisture content of commercial spaghetti used was determined as 10.2 kg water/100 kg spaghetti. The onset, peak, and end of the glass transition were determined from the shift in the DSC thermogram. Table 1 shows the onset of glass transition as a function of heating rate; it is known that the glass transition increased reverse exponentially and reached to a constant value of 55.4°C (average values at and above 30°C/min heating rate). Similar exponential rise and a constant value of 55.0°C after critical heating rate

Table 1 Effect of heating rate on the glass transition at moisture content 10.2 kg/100 kg spaghetti

Heating rate (°C/min)	T_{gi} (°C)	T_{gp} (°C)	T_{ge} (°C)
2	42.8	44.1	45.3
5	41.3 (0.9)	46.6 (3.4)	52.0 (5.3)
10	46.2	54.4	57.9
15	45.5	51.0	55.6
20	48.9	60.6	65.0
25	51.6 (0.4)	56.4 (0.3)	63.4 (1.4)
30	57.5	63.9	68.2
35	50.3 (3.7)	60.8 (0.5)	65.5 (2.8)
40	56.4	63.8	68.2
50	57.2	66.2	71.0

Values in parentheses are standard deviation

T_{gi} , T_{gp} , and T_{ei} are the onset, middle, and end of glass transition

(30°C/min) was observed by Rahman et al. (2007) in the case of other brand of commercial spaghetti (moisture content 9.8 kg water/100 kg spaghetti). For sugar solution, an exponential T_g increment was observed from 1°C/min, reaching a constant value after 10°C/min (Maurice et al. 1991), while for dates (Rahman 2004), glutenin (Cocero and Kokini 1991), and gelatin (Kasapis et al. 2003), a linear increase was observed. The higher heating rate shifts the transition to higher temperature due to the formation of stiff sample; however, it may be possible that, after a critical

heating rate, the formation of stiff sample remains the same. In addition, the observed shift in the glass transition temperature may be due to the longer time required by molecules to relax at the higher heating rate. Moreover, difference in the thermal resistance within the instrument heating plate and sample causes variation in temperature distribution in the sample as a function of heating rate.

Table 2 shows the glass transition temperature and change of specific heat at the transition as a function of water activity and moisture content. Figure 2 shows the change of onset temperature as a function of solids content. At very low water content (i.e., high solids), the glass transition temperature decreased with the decrease of solids content (solids content=100–95 kg/100 kg spaghetti). However, with further decrease of solids content up to 86 kg/100 kg spaghetti, the sample did not show further decrease in glass transition. This indicated that water could not plasticize spaghetti sample efficiently between the solids content 95 and 86 kg/100 kg spaghetti (i.e., water content=5–14 kg/100 kg spaghetti). In this region of water content (5–14 kg/100 kg spaghetti), it may remain loosely adsorbed on the solids matrix, which could be relatively free and reactive. In this case, additional water does not interact strongly with the starch or protein molecules in spaghetti, and therefore fails to decrease the T_g rapidly. The system can behave as a phase separated into water and solid. Similar results were reported by Tuyen et al. (2008) with rice samples. In the case of starch, Biliaderis et al. (1986) observed full plasticization at moisture content

Table 2 Glass transition temperature and ΔC_p for the samples containing un-freezable water

Differential scanning calorimetry (DSC)						Thermal mechanical compression (TMC)	
X_w	a_w	T_{gi} (°C)	T_{gp} (°C)	T_{ge} (°C)	ΔC_p (kJ/kgK)	X_w (kg/100kg spaghetti)	T_{g-r} (°C)
0.00	–	142.8	152.3	156.6	47		
0.87	–	130.7	139.8	145.4	64		
2.83	–	128.1	130.8	141.5	42	2.2	87.3 (4.4)
4.00	–	92.1	97.9	118.6	143	3.5	80.5 (3.7)
4.88	0.12	56.9	60.0	66.4	64	4.4	76.0 (2.4)
6.68	0.24	50.3	56.3	62.6	81	5.7	66.3 (4.4)
7.63	0.33	47.1	56.2	61.1	152		
8.48	0.45	59.5	68.4	71.6	120		
8.63	0.54	62.9	66.8	70.4	83		
9.08	0.57	55.5	62.9	66.4	114		
9.86	0.73	56.7	60.1	63.8	105		
12.99	–	38.1	44.5	54.4	69		
13.38	–	35.6	42.0	49.2	80		
13.95	0.87	42.7	48.9	48.8	87		

Heating rate 20°C/min, values in parentheses are standard deviations

X_w , water content (kg/100 kg spaghetti), a_w , water activity, ΔC_p , change of specific heat at the glass transition

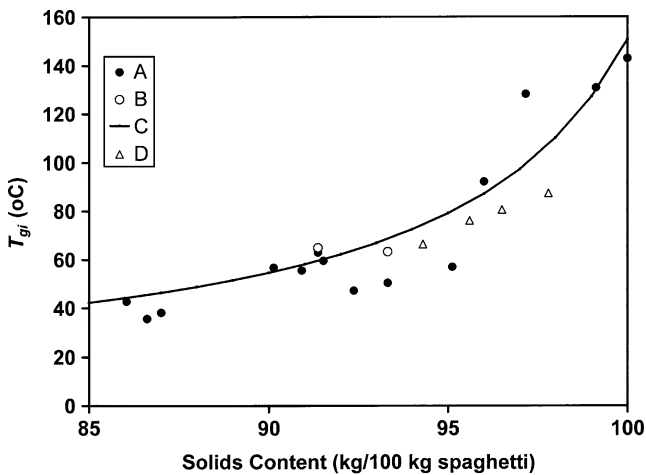


Fig. 2 A data from this study by DSC, B data from Rahman et al. (2007), C modified Gordon-Taylor model, D data from this study by TMCT

30 kg/100 kg starch, and above this level glass transition showed constant value. They proposed that, above this moisture level (i.e., maximum plasticization occurred), water formed a separate pure solvent water phase outside the starch granules. The glass transition temperatures of similar products from the literature could be compared. The glass transition temperature of starch (moisture=10.0 kg/100 kg starch) and pasta (moisture=12.5 kg/100 kg pasta) were observed at 80.0°C (Cuq et al. 2003) and 48.7°C (Takhar et al. 2006), respectively. In this study, lower values of glass transition temperatures of spaghetti were observed at 56.7 and 38.1°C, at moisture contents 9.86 and 12.99 kg/100 kg spaghetti, respectively (Table 2). This could be due to the difference in composition in spaghetti used in this study. However, the data of Rahman et al. (2007) on spaghetti measured by DSC method are comparable with the measured values in this study (see Fig. 2). The glass transition data were fitted with the modified Gordon–Taylor equation as proposed by Rahman (2009):

$$T_g = \frac{X_s T_{gs} + k_c X_w T_c}{X_s + k_c X_w} \quad (1)$$

where X_w and X_s are the water and solids content (kg/100 kg spaghetti), T_c and T_{gs} are the characteristic temperature and glass transition of solids (°C), and k_c is the modified Gordon–Taylor model parameter, respectively. The characteristic temperature (T_c) was first estimated as 7.4°C, and then T_{gs} and k_c were estimated as 150.6°C and 20.3, respectively. The model is also visually compared with the measured value in Fig. 2. Specific heat change at the glass transition did not show any trend (i.e., random variation) with the moisture content (Table 2). This random

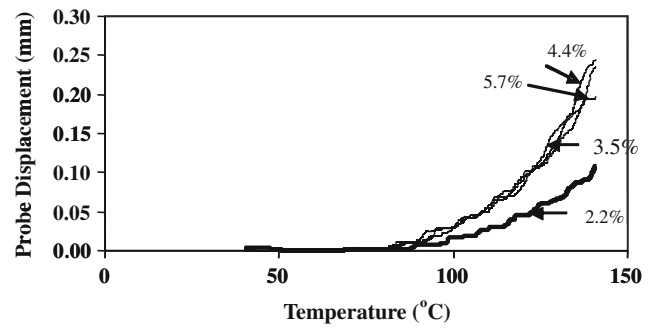


Fig. 3 Probe displacement versus temperature of spaghetti at various moisture contents

variation is relatively low (varied from 40 to 160 kJ/kg K) compared to the 768 kJ/kg K for sugar (Rahman 1995).

Figure 3 shows the displacement of spaghetti as a function of temperature measured by TMCT test method. The onset of glass transition was identified when displacement started to increase. The transition is termed as glass–rubber transition (T_{g-r}) when softening in spaghetti occurred at the interface of heating surface causing a displacement in the middle of spaghetti with applied force. The point of intersection of a linear line and tangent of the non-linear curve was considered as the onset of glass–rubber transition temperature. We found that displacement was high at higher moisture content of spaghetti since any small changes in softening of the material in contact with the device enlarged the probe displacement with the applied force at the middle. The T_{g-r} values measured at various moisture contents of spaghetti are also presented in Fig. 2 in order to compare with the results obtained by DSC. This type of variation between two methods has been previously reported (Boonyai et al. 2007; Bhandari 2007). In the cases of water contents at

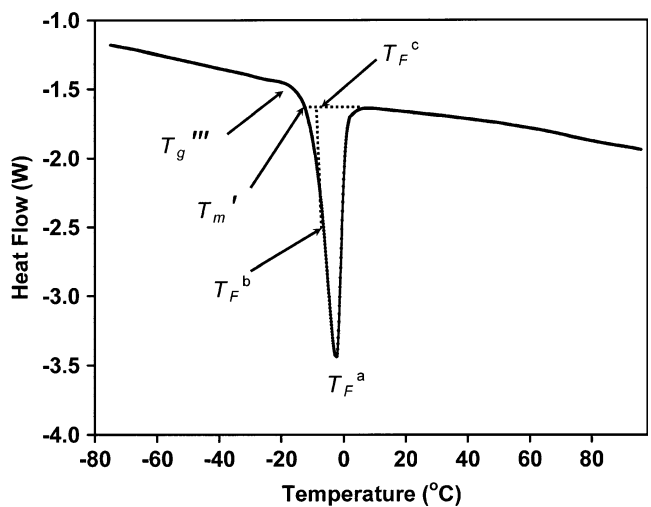


Fig. 4 DSC thermogram showing the melting endotherm for the spaghetti containing moisture content 27.0 kg/100 kg spaghetti (T_F^a , T_F^b , and T_F^c are the peak, maximum slope, and start of ice melting endotherm, and T_m' and T_g''' are the onset and end of glass transition)

Table 3 Effect of annealing [at $(T'_m)_a - 1$] on the freezing point and maximal freeze-concentration conditions

X_w	Annealing time (min)	T_F^a (°C)	T_F^b (°C)	T_F^c (°C)	ΔH (kJ/kg)	T'_m	T''_g
40	0	1.5 (1.3)	-2.2 (0.3)	-3.2 (0.1)	61 (7)	-10.8 (0.5)	-15.1 (0.5)
	30	0.4 (1.8)	-2.6 (0.2)	-4.4 (0.2)	64 (9)	-11.7 (0.3)	-15.9 (0.2)
	60	2.4 (0.4)	-2.3 (0.2)	-5.6 (4.1)	64 (6)	-10.7 (0.8)	-15.3 (0.5)
	90	1.3	-2.3	-3.3	63	-11.2	-15.3
	120	2.8	-1.9	-3.2	65	-10.0	-14.7
	150	-0.1	-2.9	-6.9	44	-10.8	-15.6
	210	2.3	-2.5	-4.4	68	-9.7	-14.4
	240	0.3	-2.7	-5.7	49	-11.3	-15.7
70	0	2.0 (0.5)	-0.7 (0.3)	-2.9 (1.1)	156 (12)	-7.0 (0.3)	-12.1 (0.2)
	30	1.8 (0.7)	-0.6 (0.5)	-3.5 (0.1)	182 (20)	-6.8 (0.0)	-11.7 (0.4)
	60	1.8	-1.1	-3.4	136	-6.5	-11.3
	90	1.6	-0.8	-3.4	145	-6.2	-10.9
	120	2.7	-0.1	-3.3	164	-6.8	-11.5
	150	1.7	-0.8	-3.5	167	-7.0	-11.4
	210	1.6	-0.6	-3.1	136	-6.2	-11.1
	240	2.2	-0.8	-3.3	137	-6.5	-11.3

Values in parentheses are standard deviations. T'_m and T''_g are the onset and end of the shift in the thermogram line before ice melting endotherm

^a Onset of ice melting endotherm

^b Maximum slope of ice melting endotherm

^c Peak of ice melting endotherm

4.88 and 6.68 kg/100 kg spaghetti, the values of TMCT showed 19.1 and 16.0°C higher values compared to DSC method, respectively, whereas in the cases of water contents 2.83 and 4.00 kg/100 kg spaghetti, TMCT showed 11.6 and 40.8°C lower values. It is usual that mechanical methods showed usually 10–20°C higher glass transition temperature (Rahman et al. 2007). As expected, TMCT method did not provide reasonably close values determined by DSC method. Displacement–temperature graph showed less displacement at moisture content 2.2 kg/100 kg spaghetti compared to higher moisture content samples (Fig. 3). This may be due to the fact that higher temperature caused a lag between the sample and heating plate used in the TMCT method or stiffer

sample with relatively low displacement. In addition, the heat loss from TMCT equipment to environment was expected to be at a higher level at higher temperature.

Figure 4 shows a typical DSC melting endotherm for spaghetti sample containing freezable water (27–70 kg/100 kg spaghetti). The baseline shift was observed just before the ice melting endotherm and considered as glass transition with the determination of onset as apparent $(T''_g)_a$ and end as apparent $(T'_m)_a$. The values of T''_g and T'_m for different annealing times (at $[(T'_m)_a - 1]$) are shown in Table 3. The results showed that there was no significant difference for annealed T''_g and T'_m as a function of annealing time (0–4 h) ($p < 0.05$). Thus, experiments were

Table 4 Freezing point and maximal freeze-concentration condition for samples containing freezable water

X_w (g/100g spaghetti)	T_F^a (°C)	T_F^b (°C)	T_F^c (°C)	ΔH (kJ/kg)	T'_m	T''_g
27	-6.2	-8.8	-10.3	2.2	-10.3	-14.0
40	1.5 (1.3)	-2.2 (0.3)	-3.2 (0.1)	60.7 (6.8)	-10.8 (0.5)	-15.1 (0.5)
60	1.8	-0.7	-2.2	106.6	-11.0	-11.5
70	2.0 (0.5)	-0.7 (0.3)	-2.9 (1.1)	155.5 (12.3)	-7.0 (0.3)	-12.1 (0.2)

Heating rate: 10°C/min. T'_m and T''_g are the onset and end of the shift in the thermogram line before ice melting endotherm. Values in parentheses are standard deviations

^a Onset of ice melting endotherm

^b Maximum slope of ice melting endotherm

^c Peak of ice melting endotherm

performed without annealing and the values T_g''' and T_m' are presented in Table 4. Tironi et al. (2009) determined the value of T_g''' as -15.2°C for sea bass fresh muscle (moisture content=76.9 kg/100 kg muscle) after annealing step at -20°C for 30 min. In the cases of bread dough at moisture content 35.1 kg/100 kg dough, Giannou and Tzia (2008) measured the $(T_g''')_a$ and $(T_m')_a$ as -25.9 and -15.8°C , respectively. These values were relatively low compared to the values found for spaghetti. However, addition of trehalose (200 ppm) in the dough shifted $(T_g''')_a$ and $(T_m')_a$ to higher values at -13.6 and -9.7°C , which is close to the results reported in this study for spaghetti. Thus, the types and additives used in the starch-based products have significant effect on the maximal freeze-concentration conditions.

The three characteristic temperatures (onset as T_F^b , maximum slope of heat flow as T_F^c , and peak as T_F^e) were determined from the endothermic peak for ice melting and are presented in Table 4. The maximal freeze-concentration condition T_m' and T_g''' (i.e., condition when maximal ice is formed from available freezable water in the spaghetti) was determined from the shift before the melting endotherm of the sample containing freezable water with lowest moisture content of 27.0 kg/100 kg spaghetti used in this experiment. The values of T_m' and T_g''' at moisture content 27.0 kg/100 kg spaghetti were found as -10.3 and -14.0°C , respectively (Table 4). Sample containing water content at 70.0 and 60.0 kg/100 kg spaghetti shifted the maximal freeze-concentration condition (i.e., T_m' and T_g''') at relatively higher temperature compared to the sample containing water content 27 and 40 kg/100 kg spaghetti. Figure 5 shows the change of freezing point and ultimate maximal freeze-concentration condition ($T_m' = -10.3^\circ\text{C}$, $T_g''' = -14.0^\circ\text{C}$, and $X_s' = 0.81$ kg/kg spaghetti) with solids content. The value of

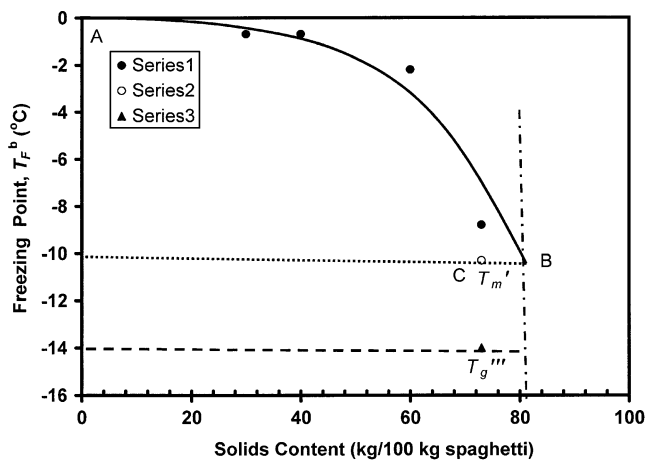


Fig. 5 Freezing point and maximal freeze-concentration condition (T_m' and T_g''') as a function of solids content for the samples containing freezable water. *Series1* freezing point, *Series2* T_m' (point C), *Series3* T_g''' , *AB* freezing curve, *B* intersection of the extended freezing curve and a horizontal line passing thru *C*

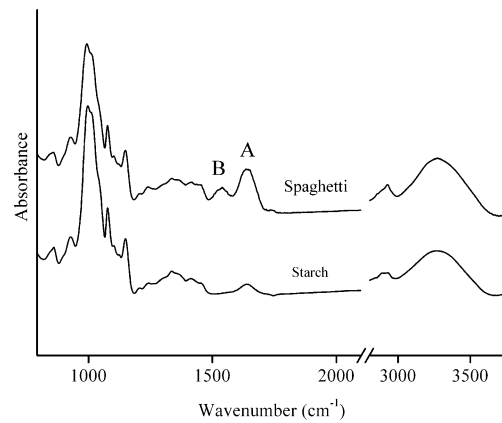


Fig. 6 FTIR spectrum for spaghetti samples containing moisture 8.5 kg/100 kg spaghetti and pure starch

X_s' was determined from the intersection (point B in Fig. 5) of the extended freezing curve AB and a horizontal line passing through T_m' (as point C in Fig. 5), and finally X_s' was read on the x -axis. The value of X_s' was found as 0.81 kg/kg spaghetti as discussed above. Thus, un-freezable water content can be estimated as $(1 - X_s')$ and the water in the right side of the vertical line passing thru B in Fig. 5 did not show any freezable water (i.e., unable to form ice even at low temperature).

Figure 6 shows the FTIR spectrum of spaghetti sample with moisture content of 8.5 kg/100 kg spaghetti. Many peaks in the spectrum were reported to represent spaghetti ingredients and many interactions within spaghetti. Bands of great importance are those assigned to characteristic groups in starch, protein, and water molecules. The hydroxyl groups and glycosidic bonds of starch are absorbed at $3,350\text{ cm}^{-1}$ (O—H stretch), $1,350\text{ cm}^{-1}$ (O—H bend), $1,150\text{ cm}^{-1}$ (C—O stretch), $1,122\text{ cm}^{-1}$

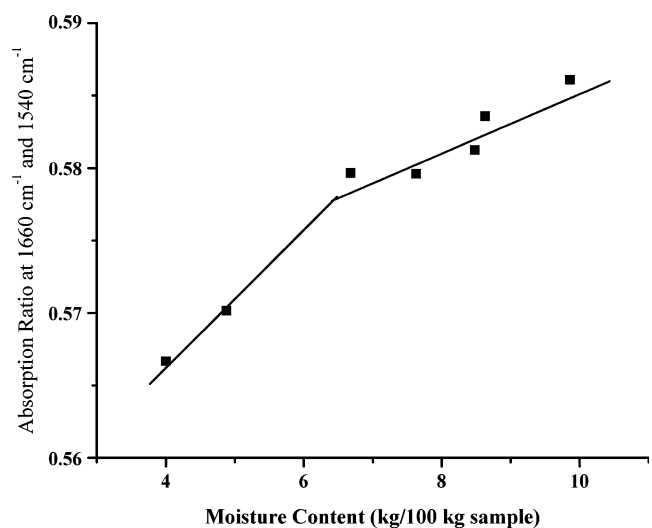


Fig. 7 Absorbance ratio at $1,660\text{ cm}^{-1}/1,540\text{ cm}^{-1}$ as a function of water contents of spaghetti

(C—C—O stretch), and 845 cm^{-1} (C—O—C stretch). On the other hand, the bands at $1,540\text{ cm}^{-1}$ (B in Fig. 6) and $1,642\text{ cm}^{-1}$ (A in Fig. 6) are assigned to the peptide bonds in protein and they are recognized as amide II (N—H bending) and amide I (C=O stretch) bands, respectively. Water is represented by two bands: O—H stretch at $3,350\text{ cm}^{-1}$ and H—O—H bending at $1,642\text{ cm}^{-1}$. The band at $1,660\text{ cm}^{-1}$ is very specific to water; however, in the case of spaghetti, the water band is very much affected by an underline absorption coming from the amide I band which is absorbed strongly in the same area. With the purpose of studying water behavior in presence of the other spaghetti molecules, the interferences coming from amide I band should be canceled. In order to do so, the traditional peak height measurement at $1,660\text{ cm}^{-1}$ was replaced with simple ratio measurement between the band $1,660\text{ cm}^{-1}$ (water+protein) and the band $1,540\text{ cm}^{-1}$ (protein).

The absorbance ratio at $1,660$ and $1,540\text{ cm}^{-1}$ as a function of moisture content in Fig. 7 shows a break at moisture content around $6.5\text{ kg}/100\text{ kg}$ spaghetti indicating the binding nature of water with solid matrix. Similarly, Fig. 2 shows a sharp increase in T_{gi} below water content $5.0\text{ kg}/100\text{ kg}$ spaghetti indicating plasticization of solid matrix. In addition, above moisture content $5.0\text{ kg}/100\text{ kg}$ spaghetti water could not plasticize the solid matrix at the same proportion compared to lower moisture content. This shows that FTIR spectrum could be used to identify the nature of water binding to the solids matrix of the spaghetti.

Conclusion

Selected phase transition properties of spaghetti were characterized by DSC and TMCT methods. The glass transition temperature measured by DSC was different from the measured ones by TMCT method due to the differences in their measurement principles. The glass transition of spaghetti was sharply decreased by the increase in the moisture content up to around $5.0\text{ kg}/100\text{ kg}$ spaghetti. Above this moisture value, the depression on the glass transition temperature with increasing moisture content was much slower. This was probably due to the weak association (binding) of water molecules with the constituents of spaghetti above moisture content $5.0\text{ kg}/100\text{ kg}$ spaghetti. This was also confirmed by the FTIR spectra which showed a point with a slope of the absorbance ratio versus moisture content line. The ultimate maximal freeze-concentration condition indicated that spaghetti contained un-freezable water of $19.0\text{ kg}/100\text{ kg}$ spaghetti. Thermal characteristics of spaghetti could be used to develop the state diagram for determining its phases, states, and storage stability as a function of temperature and moisture content.

Acknowledgments The authors would like to acknowledge the support of Sultan Qaboos University and the University of Queensland towards this research in the area of food structure. Special thanks to Dr. Moshtaque Ahmed for checking the clarity of the paper.

References

- Alvarez, M. D., Fernandez, C., & Canet, W. (2009). Oscillatory rheological properties of fresh and frozen/thawed mashed potatoes as modified by different cryoprotectants. *Food and Bioprocess Technology*, doi:10.1007/s11947-007-0051-9, in press.
- Bai, Y., Rahman, M. S., Perera, C. O., Smith, B., & Melton, L. D. (2001). State diagram of apple slices: glass transition and freezing curves. *Food Research International*, 34(2–3), 89–95.
- Bell, L. N., & Touma, D. E. (1996). Glass transition temperatures determined using a temperature-cycling differential scanning calorimeter. *Journal of Food Science*, 61(4), 807–828.
- Bhandari, B. (2007). Novel and simple technique for measuring the glass transition and melting temperature of solid food and non-food materials. SIST Annual 2007. Singapore Institute of Food Science and Technology.
- Biliaderis, C. G., Page, C. M., Maurice, T. J., & Juliano, B. O. (1986). Thermal characterization of rice starches: a polymer approach to phase transitions of granular starch. *Journal of Agricultural and Food Chemistry*, 34, 6–14.
- Boonyai, P., Howes, T., & Bhandari, B. (2007). Instrumentation and testing of a thermal mechanical compression test for glass–rubber transition analysis of food powders. *Journal of Food Engineering*, 78, 1333–1342.
- Chittur, K. K. (1998). FTIR/ATR for protein adsorption to biomaterial surfaces. *Biomaterials*, 19, 357–369.
- Cocero, A. M., & Kokini, J. L. (1991). The study of the glass transition of glutenin using small amplitude oscillatory rheological measurements and differential scanning calorimetry. *Journal of Rheology*, 35(2), 257–270.
- Cremer, D. R., & Kaletunc, G. (2003). Fourier transform micro-spectroscopic study of the chemical microstructure of corn and oat flour-based extrudates. *Carbohydrate Polymers*, 52, 53–65.
- Cuq, B., Goncalves, F., & Mas, J. F. (2003). Effects of moisture content and temperature of spaghetti on their mechanical properties. *Journal of Food Engineering*, 59(1), 51–60.
- Fabian, H., & Schultz, C. P. (2000). Fourier transform infrared spectroscopy in peptide and protein analysis. In R. A. Meyers (Ed.), *Encyclopedia of Analytical Chemistry* (pp. 5779–5803). Chichester: Wiley.
- Giannou, V., & Tzia, C. (2008). Cryoprotective role of exogenous trehalose in frozen dough products. *Food and Bioprocess Technology*, 1, 276–284.
- Jaya, S., & Das, H. (2009). Glass transition and sticky point temperatures and stability/mobility diagram of fruit powders. *Food and Bioprocess Technology*, 2, 89–95.
- Kasapis, S., Al-Mathoobi, I. M., & Mitchell, J. R. (2003). Testing the validity of comparisons between the rheological and calorimetric glass transition temperatures. *Carbohydrate Research*, 338, 787–794.
- Kazemzadeh, M., Aguilera, J. M., & Rhee, K. C. (1982). Use of microscopy in the study of vegetable protein texturization. *Food Technology*, 36(4), 111–118.
- Levine, H., & Slade, L. (1986). A polymer physico-chemical approach to the study of commercial starch hydrolysis products (SHPs). *Carbohydrate Polymer*, 6, 213–244.
- Martins, R. C., Lopes, V. V., Vicente, A. A., & Teixeira, J. A. (2008). Computational shelf-life dating: Complex systems approaches to

- food quality and safety. *Food and Bioprocess Technology*, 1, 207–222.
- Maurice, T. J., Asher, Y. J., & Thompson, S. (1991). In H. Levine, L. Slade (Eds.) *Water relationships in food*. New York: Plenum, pp. 215–233.
- Rahman, M. S. (1995). *Food properties handbook*. Boca Raton: CRC.
- Rahman, M. S. (2004). State diagram of date flesh using differential scanning calorimetry (DSC). *International Journal of Food Properties*, 7(3), 407–428.
- Rahman, M. S. (2006). State diagram of foods: its potential use in food processing and product stability. *Trends in Food Science and Technology*, 17, 129–141.
- Rahman, M. S. (2009). Food stability beyond water activity and glass transition: macro–micro region concept in the state diagram. *International Journal of Food Properties*, 12(4), 726–740.
- Rahman, M. S. (2010). Food stability determination by macro–micro region concept in the state diagram and by defining a critical temperature. *Journal of Food Engineering* (in press).
- Rahman, M. S., & Sablani, S. S. (2009). Water activity measurement methods of foods. In M. S. Rahman (Ed.), *Food Properties Handbook* (2nd ed., pp. 9–32). Boca Raton: CRC.
- Rahman, M. S., Al-Marhubi, I. M., & Al-Mahrouqi, A. (2007). Measurement of glass transition temperature by mechanical (DMTA), thermal (DSC and MDSC), water diffusion and density methods: a comparison study. *Chemical Physics Letters*, 440, 372–377.
- Roos, Y. H. (1995). *Phase transitions in foods* (p. 360). San Diego: Academic.
- Sablani, S. S., Shrestha, A. K., & Bhandari, B. R. (2008). A new method of producing date powder granules: physicochemical characteristics of powder. *Journal of Food Engineering*, 87, 416–421.
- SAS. (2001). *The SAS System for Windows, Version 8.02*, SAS Institute: Cary, NC.
- Slade, L., & Levine, H. (1988). Non-equilibrium behavior of small carbohydrate–water systems. *Pure Applied Chemistry*, 60, 1841–1864.
- Slade, L., & Levine, L. (1991). A food polymer science approach to structure property relationships in aqueous food systems: non-equilibrium behavior of carbohydrate–water systems. In H. Levine & L. Slade (Eds.), *Water relationships in food* (pp. 29–101). New York: Plenum.
- Takhar, P. S., Kulkarni, M. V., & Huber, K. (2006). Dynamic viscoelastic properties of pasta as a function of temperature and water content. *Journal of Texture Studies*, 37(6), 696–710.
- Tironi, V., Lamballeric-Anton, M., & Le-Bail, A. (2009). DSC determination of glass transition temperature on sea bass (*Dicentrarchus labrax*) muscle: effect of high-pressure processing. *Food and Bioprocess Technology*, doi:10.1007/s11947-007-0041-y, in press.
- Tuyen, T.T., Fukai, S., Truong, V., & Bhandari, B. (2008). Measurement of glass–rubber transition temperature of rice by thermal mechanical compression test (TMCT). *International Journal of Food Properties* (in press).
- van Dijk, A., De Boef, E., Bekkers, A., Van Wijk, L., Swieten, E., Hamer, R., et al. (1997). Structure characterization of central repetitive domain of high molecular weight gluten proteins. II. Characterization in solution and in the dry state. *Protein Science*, 6, 649–656.
- Wetzel, D. L. (1993). Molecular mapping of grain with a dedicated integrated Fourier transformed infrared microspectrometer. In: G. Charalambous (Ed.) *Food flavors, ingredients and composition*. Amsterdam: Elsevier, p. 679